MOLECULAR AND CELLULAR BIOLOGY, Feb. 1989, p. 726–738
0270-7306/89/020726-13$02.00/0

Vol. 9, No. 2

The Regulated Production of μ_m and μ_s mRNA Is Dependent on the Relative Efficiencies of μ_s Poly(A) Site Usage and the Cμ4-to-M1 Splice

MARTHA L. PETERSON AND ROBERT P. PERRY*

Institute for Cancer Research, Fox Chase Cancer Center, 7701 Burholme Avenue, Philadelphia, Pennsylvania 19111

Received 11 August 1988/Accepted 16 November 1988

The relative abundance of the mRNAs encoding the membrane (μ_m) and secreted (μ_s) forms of immunoglobulin μ heavy chain is regulated during B-cell maturation by a change in the mode of RNA processing. Current models to explain this regulation involve either competition between cleavage-polyadenylation at the proximal (μ_s) poly(A) site and cleavage-polyadenylation at the distal (μ_m) poly(A) site [poly(A) site model] or competition between cleavage-polyadenylation at the μ_s poly(A) site and splicing of the Cμ4 and M1 exons, which eliminates the μ_s site (μ_s site-splice model). To test certain predictions of these models and to determine whether there is a unique structural feature of the μ_s poly(A) site that is essential for regulation, we constructed modified μ genes in which the μ_s or μ_m poly(A) site was replaced by other poly(A) sites and then studied the transient expression of these genes in cells representative of both early- and late-stage lymphocytes. Substitutions at the μ_s site dramatically altered the relative usage of this site and caused corresponding reciprocal changes in the usage of the μ_m site. Despite these changes, use of the proximal site was still usually higher in plasmacytomas than in pre-B cells, indicating that regulation does not depend on a unique feature of the μ_s poly(A) site. Replacement of the distal (μ_m) site had no detectable effect on the usage of the μ_s site in either plasmacytomas or pre-B cells. These findings are inconsistent with the poly(A) site model. In addition, we noted that in a wide variety of organisms, the sequence at the 5′ splice junction of the Cμ4-to-M1 intron is significantly different from the consensus 5′ splice junction sequence and is therefore suboptimal with respect to its complementary base pairing with U1 small nuclear RNA. When we mutated this suboptimal sequence into the consensus sequence, the μ mRNA production in plasmacytoma cells was shifted from predominately μ_s to exclusively μ_m. This result unequivocally demonstrated that splicing of the Cμ4-to-M1 exon is in competition with usage of the μ_s poly(A) site. A key feature of this regulatory phenomenon appears to be the appropriately balanced efficiencies of these two processing reactions. Consistent with predictions of the μ_s site-splice model, B cells were found to contain μ_m precursor RNA that had undergone the Cμ4-to-M1 splice but had not yet been polyadenylated at the μ_m site.

The mRNAs encoding the membrane-bound (m) and secreted (s) forms of IgM heavy chain (μ) are produced from a single primary transcript which is alternatively processed at its 3′ end. If the primary transcript is cleaved and polyadenylated at the proximal (μ_s) poly(A) site, μ_s mRNA is produced. If instead it undergoes splicing of the Cμ4 and M1 exons, which removes the proximal poly(A) site, and is cleaved and polyadenylated at a distal (μ_m) poly(A) site, it gives rise to μ_m mRNA. The relative abundance of these two mRNAs is regulated during B-cell maturation, the μ_m mRNA being predominant in early stages and the μ_s mRNA being heavily favored in mature plasma cells (2, 15).

The differential expression of μ_m and μ_s mRNAs could potentially be regulated at several levels, including (i) transcriptional termination, if polymerase terminates before reaching the μ_m site, (ii) mRNA stability, if either of the mRNAs were preferentially destabilized in a stage-specific manner, and (iii) RNA processing, if any of the processing events were in direct competition with each other. Although transcriptional termination contributes to the $\mu_s \gg \mu_m$ phenotype in some plasmacytomas, it clearly does not do so in all cells exhibiting this phenotype (13, 18, 22, 23, 27, 40, 57), and therefore cannot be a primary determinant of the regulatory mechanism. The relative stability of μ_s and μ_m mRNA does not vary significantly during B-cell maturation, since similar amounts of μ_s and μ_m mRNA accumulate when μ genes capable of producing only the μ_s or μ_m transcript are transiently coexpressed in lymphoid cell lines representative of early and late developmental stages (37). This finding also indicates that linkage of the μ_s and μ_m termini is critical to the regulation. The requirement for linkage and the inability of transcriptional termination or mRNA stability to account for regulated μ_s and μ_m production both suggest that regulation of alternative RNA-processing reactions is the principal determinant.

Despite intensive efforts to define the developmentally regulated processing reactions and to understand the mechanisms by which they are controlled, a generally accepted model for this phenomenon has not yet emerged. Previous studies of the transient expression of μ genes containing modified 3′ ends have led to two somewhat different models. According to one view (18, 19), competition for cleavage-polyadenylation at the μ_s and μ_m poly(A) sites determines the fate of the mRNA precursor. This poly(A) site model supposes that splicing of the Cμ4 and M1 exons can occur only after cleavage-polyadenylation at the μ_m site and that this splicing reaction is automatically favored over cleavage-polyadenylation at the μ_s site in the μ_m-terminated precursors. The other model (37, 50, 51) considers that the fate of the mRNA precursor is mainly determined by competition

* Corresponding author.

between cleavage-polyadenylation at the μ_s site and the Cμ4-to-M1 splicing reaction. This μ_s site-splice model assumes that splicing can occur either before or after cleavage-polyadenylation at the μ_m site. Both models predict that regulation should depend on the efficiency of usage of the μ_s poly(A) site (13). However, a dependence on the efficiency of cleavage-polyadenylation at the μ_m site is predicted only by the poly(A) site model, and a dependence on the efficiency of the Cμ4-to-M1 splice is predicted only by the μ_s site-splice model. Furthermore, a developmental shift in overall cleavage-polyadenylation efficiency (9) might satisfy the requirements of either model, whereas a change in splicing efficiency (51) would be relevant only for the μ_s site-splice model.

The experiments presented here were designed to test certain predictions of these models and to investigate whether there is a unique structural feature of the μ_s poly(A) site that is essential for regulation. We constructed modified μ genes in which the μ_s or μ_m poly(A) site was replaced by other poly(A) sites and then studied their expression in cells representative of both early- and late-stage lymphocytes. The influence of these substitutions was also examined in genes bearing a deletion in the Cμ4-to-M1 intron, which markedly enhances μ_m mRNA production (18, 37, 52). The results of these experiments were more readily accommodated by the μ_s site-splice model than by the poly(A) site model. Moreover, they indicated that it is the strength of the μ_s poly(A) site, rather than a unique structure, which is important for regulation. In addition, we mutated the suboptimal 5′ splice junction sequence of the Cμ4-to-M1 intron into a consensus 5′ splice junction sequence and observed that the splice reaction dominated over polyadenylation at μ_s, even in cells which normally produce predominately μ_s mRNA. This fulfilled the prediction of the μ_s site-splice model that regulation is dependent on the Cμ4-to-M1 splicing efficiency. The μ_s site-splice model was further supported by the observation that in early-stage B cells, a substantial proportion of the μ mRNA precursor undergoes Cμ4-to-M1 splicing prior to cleavage-polyadenylation at the μ_m site.

MATERIALS AND METHODS

Plasmid constructions. To reconstruct the intact immunoglobulin genes, the plasmid pR-SP6 (35) was digested with *Bam*HI, which removed the 3′ portion of Cμ sequences. This fragment was replaced with a *Bam*HI-*Bgl*II fragment which contained the altered Cμ sequences from each of the chimeric genes (37) (Fig. 1B).

To construct the μ_s poly(A) site substitutions, several sequential cloning steps were required. The *Pst*I fragment containing the μ_s poly(A) site, μ_m splice junctions, and either the intact or shortened intron (Fig. 2A) was subcloned into pUC9 from which the *Hin*dIII site had been deleted. A *Hin*dIII-partial *Hae*II digest removed the μ_s poly(A) site, and an *Xba*I linker was inserted to maintain a restriction site. The following poly(A) fragments were then blunt-end ligated into the *Xba*I site, which had been filled in with the Klenow enzyme: a 199-base-pair (bp) *Rsa*I fragment from μ_m, a 180-bp *Dpn*I-*Hin*dIII fragment from α_s (53), and a 237-bp *Dpn*I fragment from simian virus 40 (SV40) (38) (Fig. 2B). These fragments were chosen to maintain a length of sequence upstream and downstream of the poly(A) site similar to that of the deleted poly(A) site. The correct clones were characterized by detailed restriction analysis. *Apa*I-*Kpn*I fragments containing the substituted poly(A) sites were subcloned in *Apa*I-*Kpn*I-cut pSV2Cμ (pSV5C$\mu_{s\text{-}m}$ without the polyomavirus insert [37]). The 6-kilobase (kb) *Bgl*II fragment was then cloned into pSV5*neo* to create plasmids identical to pSV5C$\mu_{s\text{-}m}$ except with the substituted poly(A) sites.

To construct the μ_m poly(A) site substitutions, the *Kpn*I-*Dra*I fragment containing the μ_m exons was subcloned into pUC18. A *Hin*cII digest removed the μ_m poly(A) site; fragments containing the α_s and SV40 poly(A) sites described above and a 278-bp *Hae*II-*Hin*fI fragment from μ_s were then inserted. These clones were characterized by detailed restriction analysis. *Kpn*I-*Xho*I fragments containing the substituted poly(A) sites were subcloned into *Kpn*I-*Xho*I-cut pSV2Cμ; the 6-kb *Bgl*II fragment was then cloned into pSV5*neo*.

All plasmids used in transfections were pSV5C$\mu_{s\text{-}m}$ derivatives (37) and were designated s-m, m-m (μ_m site substituted for μ_s), s-s (μ_s site substituted for μ_m), etc. Plasmids containing the 800-bp intron deletion (ΔAR [37]) are indicated by a Δ.

The 5′-SP mutation was created by using an oligonucleotide-directed mutagenesis protocol (14) starting with the pUC9 plasmid containing the *Pst*I fragment described above. The 31-bp oligonucleotide 5′-GGACAAGTCCACAGG TAAGTCCACACTGTAC-3′ was used to change three nucleotides at the 5′ splice junction. The mutation was confirmed by sequence analysis. The pSV5*neo* version of this mutation was reconstructed as described for the μ_s poly(A) site substitutions.

Cell culture and DNA transfections. Plasmacytoma S194 cells were obtained from the American Type Culture Collection and maintained in Dulbecco modified Eagle medium (GIBCO Diagnostics) containing 10% horse serum. The Abelson murine leukemia virus-transformed cell line 3-1 (3) and the B-cell lymphoma cell line 38C-13 were maintained in RPMI 1640 medium (GIBCO) containing 10% fetal bovine serum. The DEAE-dextran transfection protocol (21) was used for the transient expression assays. S194 cells were harvested 40 h after transfection; 3-1 cells were harvested 24 h after transfection. Consistent results were obtained in replicate transfection experiments with the same construct and cell line.

RNA preparation and analysis. Cytoplasmic RNA was extracted (43) and passed over oligo(dT) columns to isolate poly(A)$^+$ RNA. Nuclear RNA was extracted by the hot phenol procedure from 10^9 citric acid-purified nuclei (42, 44) and passed through an oligo(dT) column, and the poly(A)$^+$ and poly(A)$^-$ fractions were collected. The poly(A)$^-$ fraction was again passed through the oligo(dT) column. Northern (RNA) blot analysis of RNA was performed on 1.5% agarose–formaldehyde gels; the RNA was transferred to Nytran (Schleicher & Schuell, Inc.), and the filters were hybridized with nick-translated DNA fragments as detailed by Kelley et al. (24). The SV*neo* probe was a 384-bp *Bgl*I-*Bgl*II fragment from pSV2*neo*, and the polyomavirus probe was a 3.6-kb *Bam*HI fragment from pSV5*neo*.

For S1 nuclease analysis (4) of S194 transfection experiments, either total cytoplasmic RNA (100 μg) or poly(A)$^+$ cytoplasmic RNA (1 μg plus 100 μg of nonspecific carrier RNA) was hybridized to 20 to 30 ng of end-labeled double-stranded probe. S1 nuclease analysis of nuclear RNA was performed with 1 μg of poly(A)$^+$ RNA plus 100 μg of carrier RNA from plasmacytoma cells that do not express μ RNA or with 100 μg of poly(A)$^-$ RNA. The μ_s p(A)/μ_m 5′ splice probe, which distinguishes RNA cleaved at the μ_s poly(A) site from RNA spliced from Cμ4 to M1, is a 640-bp *Pst*I-

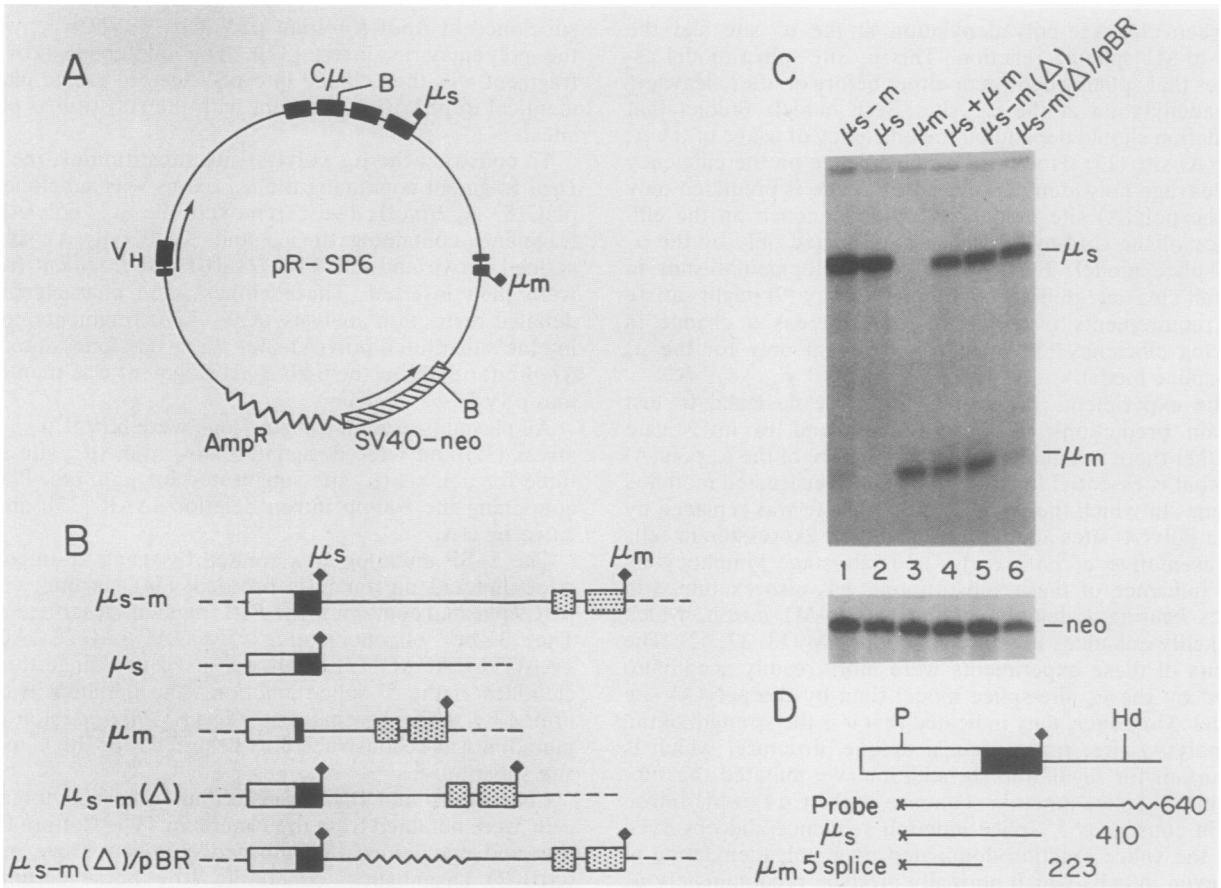

FIG. 1. Structure and expression of complete immunoglobulin μ genes containing 3′ end modifications. (A) Structure of the pR-SP6 plasmid, taken from Ochi et al. (35). Solid lines represent the genomic immunoglobulin sequence; ■, exons; ▨, SV40 and neomycin resistance gene sequences; ∿∿∿, bacterial plasmid sequences; ◆, cleavage-polyadenylation sites. Arrows show the direction of transcription. The *Bam*HI sites (B) delimit the fragment that was replaced by the corresponding region from chimeric genes originally reported by Peterson and Perry (37). (B) 3′ End structure of the μ region for each plasmid reconstructed from the chimeric genes. ▭, Segment of the Cμ4 exon that is common to both μ_s and μ_m mRNA; ■, segment specific to μ_s mRNA; ▩, exons specific to μ_m mRNA. The thin lines are intron sequences; all other symbols are as in panel A. (C) S1 nuclease analysis of total cytoplasmic RNA from S194 plasmacytoma cells transfected with the plasmids indicated above each lane. The top panel shows analysis with the μ_s poly(A)/μ_m 5′ splice probe diagrammed in panel D; protected bands are identified. The lower panel shows analysis with a probe specific for the 5′ end of the neo transcript. The relative levels of total μ transcripts, adjusted for variations in *neo* expression and normalized to the wild-type (μ_{s-m}) value, are 1.0, 1.1, 0.4, 0.8, 0.9, and 0.8 for lanes 1 to 6, respectively. (D) Diagram of the μ_s poly(A)/μ_m 5′ splice probe used for S1 nuclease analysis. The sizes (in nucleotides) of the full-length probe and protected fragments are indicated. P, *Pst*I; Hd, *Hin*dIII; other symbols are as in panels A and B.

*Eco*RI fragment containing 610 bp of Cμ sequence plus 30 bp of vector sequence (Fig. 1D); it was 3′ end labeled by using the Klenow enzyme and [α-^{32}P]dCTP. The accurate quantitation of these two RNA species with this particular probe was verified with the μ_s-and μ_m-specific S1 probes used previously (37). The *neo*-specific probe, a 520-bp *Sph*I-*Bgl*II fragment from the vector pSV2*neo* and the μ_m 3′ splice probe, a 158-bp *Ava*II fragment, were end labeled by using T4 polynucleotide kinase and [γ-^{32}P]ATP. The μ_m p(A) probe, a 291-bp *Xba*I-*Eco*RI fragment, was 3′ end labeled by using Klenow enzyme and [α-^{32}P]dCTP. The *Mbo*II-*Eco*RI portion of this probe contains sequences from the plasmid vector. Hybridization temperatures for the various probes were as follows: μ_s p(A)/μ_m 5′ splice and *neo*, 50°C; μ_m 3′ splice, 42°C; and μ_m p(A), 37°C. S1 nuclease digestion was for 30 min at 23 or 42°C. The reactions were analyzed on 4, 6, or 8% polyacrylamide–7 M urea gels. The data from both Northern blot and S1 analyses were quantitated by densitometer tracings of various autoradiographic exposures.

RESULTS

A comparison of the effects of 3′ end modifications in complete and chimeric μ genes. The transient expression system that we previously used to study μ_s and μ_m regulation employed a chimeric SV40-*neo*-Cμ gene in a plasmid vector which contained polyomavirus sequences, allowing it to replicate in mouse cells (37). We observed appropriate expression of this chimeric gene in both pre-B and plasmacytoma cell lines. However, to ensure that the effects of changes made in the 3′ Cμ region were due solely to these changes and were not dependent on the chimeric nature of the transcript or the high copy number of expressed genes, we substituted the 3′ portions of representative chimeric genes into the nonreplicating plasmid pR-SP6 (35), which contains an intact copy of the μ gene from the Sp6 hybridoma cell line (Fig. 1A and B). This plasmid contains an independent transcription unit, the *neo* gene, which can be used as a control for transfection efficiency and RNA yield.

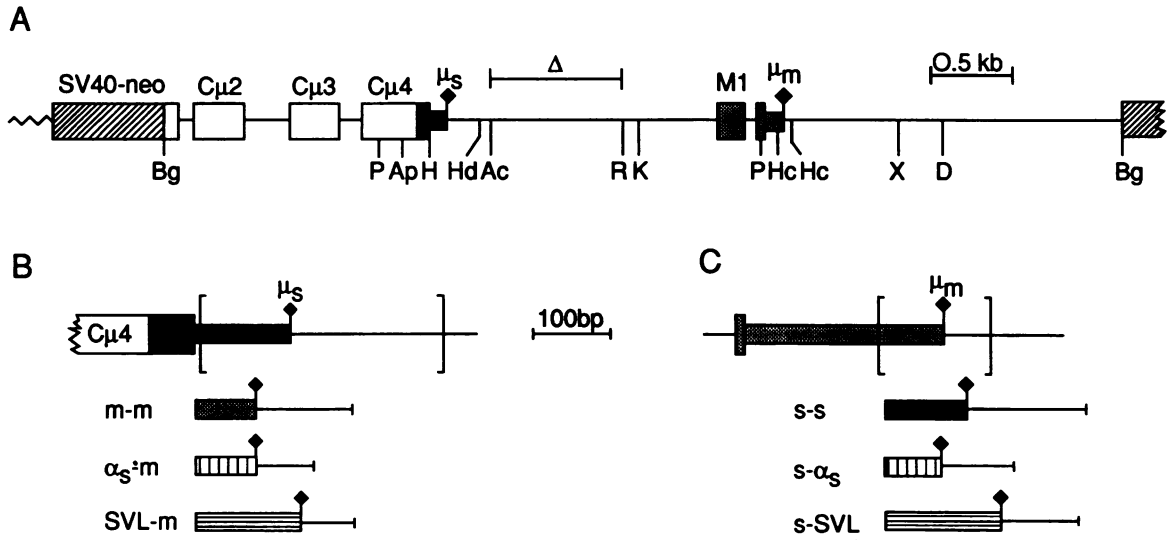

FIG. 2. Diagram of the chimeric gene and poly(A) site substitutions. (A) The chimeric SV40-*neo*-Cμ gene, drawn to scale. Symbols are as in Fig. 1; the narrow boxes denote the 3′ untranslated portions of the message. Δ denotes the portion of the intron deleted in the constructs labeled with a (Δ) in the text. Restriction sites are abbreviated as follows: Ac, *Acc*I; Ap, *Apa*I; Bg, *Bgl*II; D, *Dra*I; H, *Hae*II; Hc, *Hin*cII; Hd, *Hin*dIII; K, *Kpn*I; P, *Pst*I; R, *Eco*RI; X, *Xho*I. (B) Structures of the μ_s poly(A) site substitutions. The portion of the μ_s poly(A) site replaced is delimited by brackets; the substituted poly(A) sites and the names of the plasmids are shown below. ▭, transcribed α_s sequences; ▬, transcribed SVL sequences. (C) Structures of the μ_m poly(A) site substitutions. The portion of the μ_m poly(A) site replaced is delimited by brackets; the substituted poly(A) sites and the names of the plasmids are shown below. Symbols are as in panel B.

These immunoglobulin genes, which are otherwise intact except for the 3′ end alterations, were transiently expressed in the plasmacytoma cell line S194. This line expresses only the secreted form of immunoglobulin α-chain mRNA as judged by Northern blot and S1 nuclease analysis with a Cα probe (data not shown). The RNA from the transfected plasmids was assayed by S1 nuclease mapping with a probe that distinguishes mRNA that has been cleaved at the μ_s poly(A) site from mRNA that has undergone the Cμ4-to-M1 splice (Fig. 1D), thus enabling the ratio of μ_m-to-μ_s expression to be measured in a single S1 nuclease assay. The expression of the *neo* gene was also assayed by S1 nuclease analysis.

The relative expression of this set of complete immunoglobulin genes (Fig. 1C) was virtually identical to that previously observed with the corresponding chimeric SV40-*neo*-Cμ genes (see Fig. 2 and 4 of reference 37). Furthermore, the total amount of μ transcript expressed from each construct was relatively constant when standardized to the level of *neo* expression. The μ_s and μ_m constructs each produced one transcript (Fig. 1C, lanes 2 and 3); when cotransfected, they produced similar amounts of transcript even though the wild-type control ($\mu_{s\text{-}m}$) produced predominantly μ_s in these cells (lanes 4 and 1). The effect of the intron deletion [$\mu_{s\text{-}m}(\Delta)$] was to increase the expression of μ_m and decrease expression of μ_s (Fig. 1C, lane 5 versus lane 1). The wild-type expression pattern was observed when the intron length was restored to its original size by the insertion of pBR vector sequence (Fig. 1C, lane 6). The fact that the deletion caused reciprocal changes in μ_s and μ_m mRNA production indicates that it acts by shifting the balance between competitive RNA-processing reactions (see Discussion). Since there was essentially no difference between the results obtained with these complete genes and those obtained previously with the chimeric genes, we concluded that the 5′ end of the transcript does not affect the regulated alternative processing at the 3′ end and that differences in gene copy number or in the ability of plasmid vectors to replicate can also be ignored. The transcripts derived from the chimeric μ gene can be specifically identified with a probe for the SV40-*neo* region and can therefore be readily distinguished from the transcripts of endogenous μ genes in pre-B or B cells. Because of this advantage, we have continued to use the chimeric construct in subsequent experiments.

Substitutions at the μ_s poly(A) site. Cleavage-polyadenylation at the μ_s poly(A) site is a reaction involved in μ_s and μ_m regulation, according to both processing models. To investigate whether there are any unique features of the μ_s poly(A) site that are essential for this regulation, we replaced the μ_s site with other poly(A) sites in chimeric genes containing either full-length or shortened Cμ4-to-M1 introns and analyzed the expression of these constructs in pre-B and plasmacytoma cells. Although the intrinsic strengths of these inserted poly(A) sites may vary, these constructs could still be subject to normal regulation. If this were so, then the ratio of mRNA terminated at the μ_s or at its substituted poly(A) site (μ_s* mRNA) to μ_m mRNA should be higher in the plasmacytoma cell line S194 than in the pre-B cell line 3-1, reflecting the developmental differences between these two cell lines. The μ_s poly(A) site was deleted, leaving the μ_m poly(A) site and the rest of the 3′ end intact, and fragments containing the μ_m poly(A) site (m), the poly(A) site for the secreted form of α heavy chain (α_s), and the poly(A) site of SV40 late mRNA (SVL) were inserted in its place (Fig. 2A and B). According to our current knowledge of splicing mechanisms (47), all of the sequences necessary for efficient Cμ4-to-M1 splicing are retained in these constructs. Similarly, the substituted poly(A) sites contain all of the sequences required for proper functioning of the cleavage-polyadenylation mechanism (8). The RNA expressed from these plasmids was analyzed by both Northern blotting (Fig. 3A and C) and S1 nuclease mapping (Fig. 3B). The Northern blots were sequentially analyzed with the SV40-*neo* probe to detect the μ RNA transcripts and with a polyomavirus-specific probe to monitor transfection efficiency and RNA

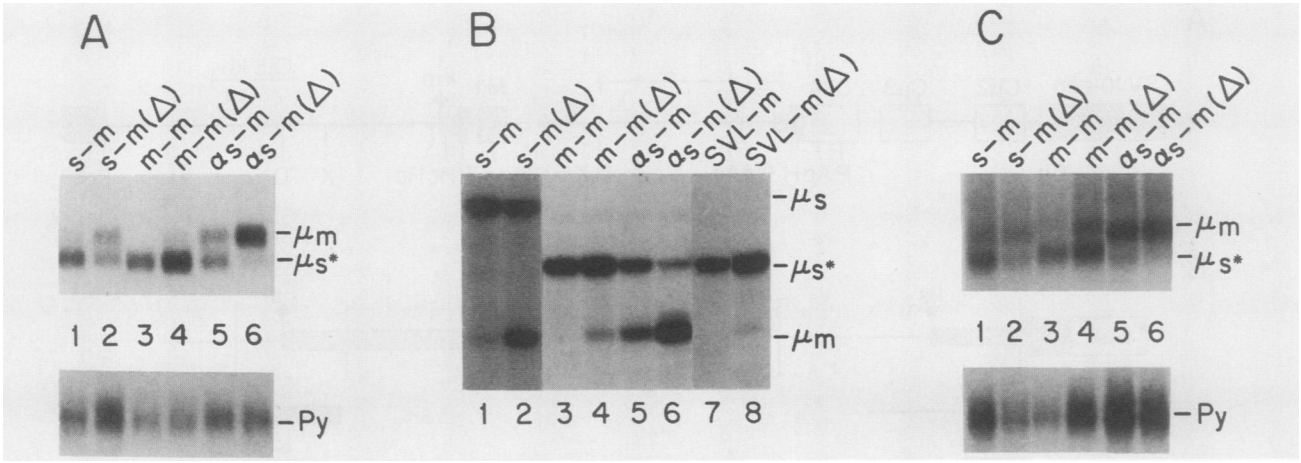

FIG. 3. Expression of the μ_s poly(A) site substitutions in the plasmacytoma S194 and the pre-B-cell line 3-1. (A) Northern blot analysis of poly(A)$^+$ RNA from S194 cells transfected with the plasmids shown above each lane. The transcripts are labeled as follows: μ_m denotes the 2.0-kb μ_m mRNA, and μ_s* denotes the ~1.8-kb mRNA cleaved and polyadenylated at the μ_s or substituted poly(A) site. The top panel was analyzed with a probe specific for SV40-*neo* sequences; the bottom panel is the same blot reprobed for polyomavirus sequences. The relative levels of total μ transcripts, adjusted for variations in polyomavirus expression and normalized to the wild-type (s-m) value, are 1.0, 0.6, 0.9, 2.0, 0.9, and 1.3 for lanes 1 to 6, respectively. (B) S1 nuclease analysis of RNA from S194 cells transfected with the plasmids shown above each lane. The S1 probe is diagrammed in Fig. 1D. μ_s and μ_m are fragments protected by μ_s mRNA and μ_m RNA, respectively. μ_s* are the fragments protected by mRNA cleaved and polyadenylated at the substituted poly(A) sites. These fragments are uniformly 297 bp, which is the extent of homology between the probe and the RNA. (C) Northern blot analysis of poly(A)$^+$ RNA from 3-1 cells transfected with the plasmids shown above each lane. The transcripts are labeled as in panel A. The top panel was analyzed with a probe specific for SV40-*neo* sequences; the bottom panel is the same blot reprobed for polyomavirus sequences. The relative levels of μ transcripts, adjusted for variations in polyomavirus expression and normalized to the wild-type value, are 1.0, 1.1, 1.5, 1.2, 0.7, and 0.9 for lanes 1 to 6, respectively. The SVL-m and SVL-m(Δ) constructs were not analyzed on Northern blots because the μ_s* transcripts could not be adequately separated from the μ_m transcripts on the basis of size.

yield. When the μ_m site was substituted for μ_s in both plasmacytoma and pre-B cells, this substituted site was used exclusively, indicating that the μ_m site constitutes a very strong cleavage-polyadenylation signal (Fig. 3A-C, lanes 3). However, with the intron deletion, which favors the competing μ_m-processing reaction, the ratio of μ_s* to μ_m transcripts was clearly higher in the plasmacytoma cells than in pre-B cells (Fig. 3C, lane 4, versus Fig. 3A and B, lane 4; Table 1). Therefore, under these conditions, constructs containing the μ_m poly(A) site substituted for μ_s could be regulated. The SV40 late poly(A) site, when substituted for μ_s, showed an expression pattern similar to that of the μ_m poly(A) site (Fig. 3B; compare lanes 7 and 8 with lanes 3 and 4). Regulation was observed both with and without the intron deletion when the α_s site was substituted for μ_s, although relatively more μ_m was produced from these constructs than from those containing the μ_s site (Fig. 3A and B, lanes 5 and 6, versus Fig. 3C, lanes 5 and 6; Table 1). The fact that none of the substituted sites abolished the developmental regulation, although each affected the expression ratio, indicates that no structural feature unique to the μ_s poly(A) site is required for regulation. Rather, these results suggest that the relative strength of the μ_s poly(A) site is the critical parameter. On the basis of the observed ratios of μ_m and μ_s* mRNA, we would order the poly(A) site strengths or efficiencies as SVL $\approx \mu_m > \mu_s > \alpha_s$, with a total range of more than 100-fold.

TABLE 1. Effect of substitutions at the μ_s poly(A) site

Construct	μ_s* RNA/μ_mRNA in[a]:		Regulation index (plasmacytoma/ pre-B cell)
	Pre-B cells	Plasmacytoma cells	
s-m (wild type)	1.5 ± 0.2	11 ± 4	7
m-m	>100	>100	
α_s-m	0.22 ± 0.06	1.4 ± 0.1	6
s-m (Δ)	0.6 ± 0.09	1.2 ± 0.3	2
m-m (Δ)	1.7 ± 0.2	17 ± 3	10
α_s-m (Δ)	0.05 ± 0.01	0.08 ± 0.02	2

[a] Values are the means ± standard deviations of from three to five independent experiments.

These results also demonstrate that the proper balancing of processing reaction efficiencies is critical for this type of regulatory mechanism. Although the μ_s poly(A) site substitutions did not abolish regulation, the magnitude of the difference in expression between pre-B and plasmacytoma cells varied among the different constructs (Table 1). Those exhibiting the greatest difference were s-m (wild-type), m-m(Δ), and α_s-m, while the expression difference of s-m(Δ) and α_s-m(Δ) was only about twofold and could not be measured for m-m. This indicates that the efficiencies of the competing processing reactions must be delicately balanced in order for these reactions to respond effectively to the developmentally controlled regulatory mechanism(s). For example, only with the strongest poly(A) site (μ_m) substituted for μ_s was regulation observed with the intron deletion-containing constructs. This suggests that the μ_m poly(A) site is optimally balanced with the deletion-enhanced competing reaction (most likely splicing, as will be discussed below), while the weaker poly(A) sites (μ_s and α_s) are not.

Although the various substitution constructs exhibit striking differences in the relative production of μ_s* and μ_m mRNA, the total levels of μ transcript produced by each construct were similar (± 30% and ± 20% for the plasmacytoma and pre-B cells, respectively [Fig. 3]). Thus, an increase or decrease in μ_s* expression was usually accompanied by a corresponding decrease or increase in μ_m expression. Such reciprocity indicates that the poly(A) site

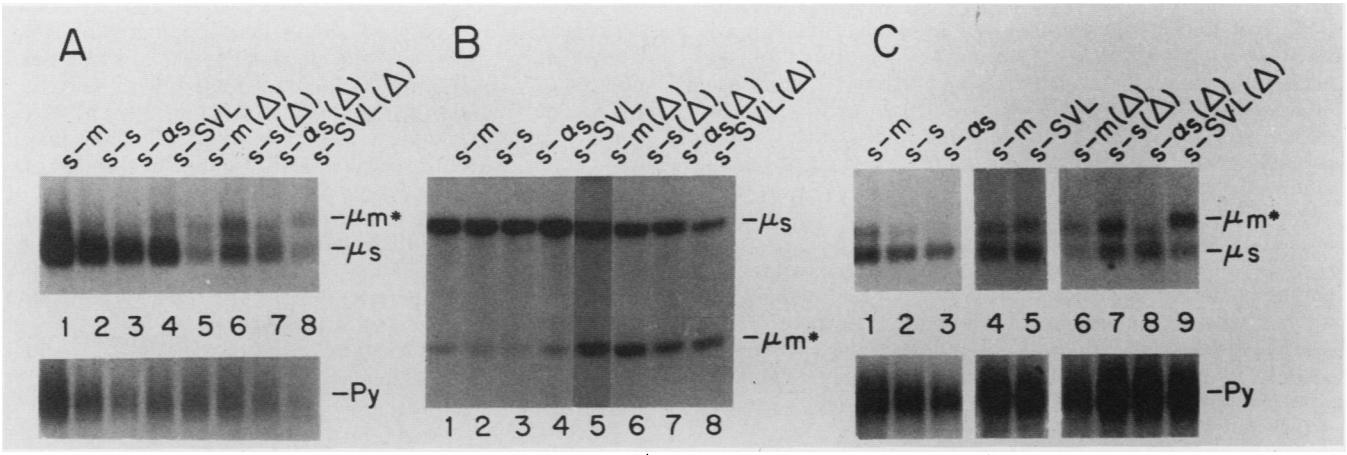

FIG. 4. Expression of the μ_m poly(A) site substitutions in the plasmacytoma S194 and the pre-B-cell line 3-1. (A) Northern blot analysis of poly(A)$^+$ RNA from S194 cells transfected with the plasmids shown above each lane. The transcripts are labeled as follows: μ_s denotes the 1.8-kb μ_s mRNA, and μ_m* denotes the ~2.0-kb mRNA cleaved and polyadenylated at either the μ_m site or the substituted poly(A) site. The top panel was analyzed with a probe specific for SV40-*neo* sequences; the bottom panel is the same blot reprobed for polyomavirus sequences. The relative levels of μ transcripts, calculated as in Fig. 3, are 1.0, 0.7, 1.0, 0.8, 0.3, 0.9, 0.9, and 0.8 for lanes 1 to 8, respectively. (B) S1 nuclease analysis of RNA from S194 cells transfected with the plasmids shown above each lane. The S1 probe is diagrammed in Fig. 1D; transcripts are labeled as in panel A. (C) Northern blot analysis of poly(A)$^+$ RNA from 3-1 cells transfected with the plasmids shown above each lane. The transcripts are labeled as in panel A. Lanes 1 to 3, lanes 4 and 5, and lanes 6 to 9 are from three separate experiments. The top panel was analyzed with a probe specific for SV40-*neo* sequences; the bottom panel is the same blot reprobed for polyomavirus sequences. The levels of transcripts for s-s, s-α_s, and s-SVL corrected for variations in polyomavirus expression and normalized to the values for s-m are 1.0, 1.0, and 1.2 for μ_s RNA and 0.4, 0.2, and 1.0 for μ_m* RNA. The corrected levels of transcripts for s-α_s(Δ) and s-SVL(Δ) normalized to s-s(Δ) are 1.3 and 0.7 for μ_s RNA and 0.6 and 1.6 for μ_m* RNA. In this experiment, the transcript levels for s-m(Δ) were too low for accurate quantitation.

substitutions, as well as the intron deletions, act by shifting the balance between competing RNA-processing reactions.

Substitutions at the μ_m poly(A) site. To determine whether the μ_m poly(A) site is in competition with the μ_s poly(A) site, as predicted by the poly(A) site model, we replaced the μ_m poly(A) site with each of the poly(A) sites used in the μ_s substitution experiments (Fig. 2C). These sites differed by up to 200-fold in their relative strengths when substituted at the μ_s poly(A) site position. If the μ_m and μ_s poly(A) sites were in direct competition, then replacing μ_m with a weaker site should decrease the level of transcript cleaved and polyadenylated at this distal (μ_m*) site and concomitantly increase the amount of μ_s transcript. Contrary to this prediction, substitutions at the μ_m* poly(A) site had very little effect on the relative production of μ_m* and μ_s mRNA when these genes were transfected into plasmacytoma cells (Fig. 4A and B; Table 2). This is most obvious in the presence of the shortened intron (Fig. 4A and B, lanes 5 to 8); when the α_s poly(A) site was substituted for the μ_m site, the expression ratio differed by less than twofold. This is in contrast to the 30- to 200-fold difference seen between these two poly(A) sites when substituted for the μ_s site. These results clearly favor the μ_s site-splice model over the poly(A) site model.

The expression of this set of constructs in the pre-B cells was different from that in plasmacytoma cells. In pre-B cells, substitutions of weaker poly(A) sites at the μ_m site caused a reduction in the level of μ_m* mRNA, although this reduction was not accompanied by a compensatory increase in μ_s transcripts, as would be expected if these reactions were in direct competition (Fig. 4C, lanes 1 to 5; Table 2). A similar effect was observed with the intron deletions (Fig. 4C, lanes 6 to 9). Instead of alteration of the balance between the two competing processing reactions, as was seen with the μ_s substitutions, it seemed that another event related to total mRNA yield was affected. For example, substitution of the μ_m poly(A) site with weaker poly(A) sites could lead to greater transcript wastage if nonpolyadenylated mRNA precursors were more vulnerable to degradation than their polyadenylated counterparts. It is noteworthy that this effect is evident in pre-B cells but not in plasmacytoma cells. This difference in response to variation of poly(A) site strength could be explained if the overall cleavage-polyadenylation efficiency were lower in pre-B cells than in plasmacytoma cells, in which case the effect of a weaker poly(A) site might be more dramatic. Alternatively, the degradation process might be more efficient in the pre-B cells.

5′ Splice site mutation. To test directly the involvement of the Cμ4-to-M1 splice, we constructed a splice junction mutation that should increase the efficiency of this splicing reaction. When we compared the 5′ splice junction sequences of the Cμ4-to-M1 intron from a number of species, including mouse, human, hamster, chicken, toad, and shark, with sequences of the analogous splice junctions from the other mouse heavy-chain isotypes, which also produce secretory and membrane forms of immunoglobulin, we no-

TABLE 2. Effect of substitution at the μ_m poly(A) site

Contruct	μ_s RNA/μ_m* RNA in[a]:	
	Pre-B cells	Plasmacytoma cells
s-m (wild-type)	2.0 ± 0.6	11
s-s	5 ± 0.5	11
s-α_s	10 ± 1	11
s-SVL	2.5 ± 0.6	11
s-m (Δ)	0.6 ± 0.03	1.2
s-s (Δ)	0.8 ± 0.07	1.4
s-α_s (Δ)	1.8 ± 0.2	2.2
s-SVL (Δ)	0.4 ± 0.03	1.2

[a] Pre-B-cell values are means ± standard deviations of two to four independent experiments; plasmacytoma cell values are from a single experiment.

ticed that there were several striking similarities (Fig. 5). First, the nucleotide at +5 from the splice junction was almost always an A and never a G, which is the consensus nucleotide at this position (Fig. 5A, B). In fact, a G at +5 occurs in 82% of splice junctions (46) and is the site of a β-thalassaemia mutation which decreases correct splicing while increasing the use of cryptic splice sites (49). Also, in adenovirus, a double mutation at +5 and +6 severely impairs proper splicing (48). Although position +5 is part of the Cμ4-to-M1 intron, this nucleotide is also within the coding region for μ_s protein, raising the possibility that there are coding requirements for this sequence. However, the A at +5 is the third base of the AAA codon for lysine (Fig. 5C); a G at this position would not change the coding capacity, since AAG also codes for lysine. These two codons are used with about equal frequency throughout the μ gene, and therefore the absence of a G at position +5 cannot be attributed to coding sequence constraints.

A second feature of this 5′ splice junction is that the nucleotide at the −2 position, which is an A in 56% of 5′ splice junctions (46), was never an A in these splice junctions, although all other nucleotides were represented. Third, the consensus U at the +6 position was present only in the splice junctions from the γ genes and is a C, A, or G in the others. The sequences of other 5′ splice junctions within the μ gene were more divergent and did not resemble this particular 5′ splice junction sequence (Fig. 5B). Finally, the strong evolutionary conservation of this sequence did not extend to neighboring sequences (Fig. 5C).

Splice junctions which are more similar to the consensus sequence and which therefore can base pair more strongly with U1 small nuclear RNA (Fig. 5B) have been shown to be stronger, more efficient splice junctions (16, 59). Therefore, we mutated the 5′ splice junction of the Cμ4-to-M1 intron by using oligonucleotide-directed mutagenesis to create a consensus splice junction (Fig. 6A) and expressed this construct (5′-SP) in the plasmacytoma cell line S194, in which the production of μ_s mRNA is normally greatly favored. The striking result was that only the spliced μ_m mRNA was produced from the 5′-SP construct (Fig. 6B and C), indicating that splicing of the improved splice junction was completely dominant over the normally very efficient cleavage-polyadenylation of the μ_s poly(A) site. This result unequivocally demonstrates that splicing of the Cμ4-to-M1 intron is in competition with the μ_s cleavage-polyadenylation reaction.

Analysis of μ_m mRNA precursors. The experiments presented above strongly support a model for regulated production of μ_s and μ_m mRNA wherein cleavage-polyadenylation at the μ_s poly(A) site competes with the splice between the Cμ4 and M1 exons. According to this model, the splicing efficiency is a major determinant of the μ_m/μ_s ratio and is not dependent on prior cleavage-polyadenylation at the μ_m poly(A) site. If this is the case, one would predict that in pre-B or B cells, in which μ_m mRNA is the predominant species, there might be a significant accumulation of nonpolyadenylated μ mRNA precursor that has already undergone the Cμ4-to-M1 splice. To establish the existence of such a precursor, we used S1 nuclease protection analysis to assay the poly(A)$^-$ fraction of nuclear RNA from a B-cell line, 38C-13, which produces μ_m and μ_s mRNA at a ratio of about 2:1 (33). S1 mapping across both splice junctions and both poly(A) sites was done on poly(A)$^+$ as well as poly(A)$^-$ nuclear RNA fractions. With the μ_s p(A)/μ_m 5′ splice probe, the poly(A)$^+$ RNA fraction protected two fragments which corresponded to mature μ_m and μ_s mRNA in a ratio of about 2:1 (Fig. 7A). The poly(A)$^-$ RNA did not contain any RNA cleaved at the μ_s poly(A) site, as was expected from a clean poly(A)$^-$ RNA fraction not contaminated with poly(A)$^+$ RNA. This fraction, however, did protect a fragment which corresponded to an unprocessed transcript (RT) as well as a fragment which corresponded to RNA that has undergone the Cμ4-to-M1 splice. By quantitating the relative amount of spliced RNA present in the poly(A)$^+$ and poly(A)$^-$ RNA fractions and taking into account the yield of poly(A)$^+$ RNA, we can estimate the abundance of spliced poly(A)$^-$ RNA relative to spliced poly(A)$^+$ RNA (mature μ_m mRNA) present in the nucleus. The ratio of spliced poly(A)$^-$ RNA to spliced poly(A)$^+$ RNA, on the basis of multiple determinations of several 38C-13 nuclear RNA preparations, is 0.22 ± 0.08.

To verify that the RNA which this probe detected as being processed at the 5′ splice junction was indeed spliced to the 3′ splice junction and was not simply an incompletely spliced intermediate or an aberrantly spliced RNA, we analyzed the same preparation of 38C-13 RNA for transcripts spliced at the 3′ splice junction of the Cμ4-to-M1 intron (Fig. 7B). The ratio of spliced poly(A)$^-$ to poly(A)$^+$ RNA detected with the μ_m 3′ splice junction probe was similar to that detected with the 5′ splice probe, indicating that most of these RNA species were correctly spliced. Using a probe which detected RNA cleaved at the μ_m poly(A) site (Fig. 7C), we found none of this RNA in the poly(A)$^-$ fraction, providing further evidence that the spliced RNA we detected had not been previously cleaved and polyadenylated.

Consistent with this spliced, nonpolyadenylated RNA being a precursor to μ_m mRNA, when 38C-13 cells were treated with actinomycin D under conditions that chase poly(A)$^+$ precursors to product (43, 54), the level of this RNA decreased by about half (data not shown). This suggests that at least half of this RNA could be μ_m mRNA precursor and therefore that the ratio of spliced poly(A)$^-$ precursor RNA to mature μ_m mRNA is at least 0.11. The ratio of unspliced poly(A)$^+$ μ_m mRNA precursor to mature μ_m mRNA, judged by a Northern blot analysis of poly(A)$^+$ nuclear RNA similar to that presented by Nelson et al. (33), is about 0.07. If the steady-state levels of poly(A)$^-$ and poly(A)$^+$ precursors are indicative of the flux through the possible processing pathways of μ_m mRNA, then the pathway in which splicing of Cμ4 to M1 commits the precursor to becoming a mature μ_m mRNA is at least as important as one in which polyadenylation at the μ_m site precedes the splice reaction.

Other cell lines were also analyzed for the presence of this spliced poly(A)$^-$ transcript to ensure that it is a general feature of the μ_m mRNA-processing scheme and not a peculiarity of the 38C-13 cell line. The B-cell lines WEHI231 and 70Z/3 both contained this spliced precursor in a clean poly(A)$^-$ fraction of nuclear RNA (data not shown).

DISCUSSION

The combined results of the poly(A) site substitution experiments and the splice junction mutation experiment prove that μ_s and μ_m regulation is achieved by a competition between cleavage-polyadenylation at the μ_s poly(A) site and splicing of the Cμ4 and M1 exons. Since the μ_s poly(A) site could be substituted without abolishing regulation, no feature unique to this site is essential for the regulatory mechanism. However, the ratio of μ_m to μ_s* transcripts was altered when the μ_s poly(A) site was substituted; thus, the intrinsic strength of the μ_s poly(A) site, e.g., its affinity for

A

	-2	-1		+1	+2	+3	+4	+5	+6
CONSENSUS 5' SPLICE	A	G	↓	G	U	A	A	G	U
	56							82	53
		78		100	100	60	69		
	17							7	17
MOUSE μ 5' SPLICE	U	G	↓	G	U	A	A	A	C

B

U1 snRNA	U	C		C	A	U	U	C	A
	|	|		|	|	|	|	|	|
CONSENSUS	A	G	↓	G	U	A	A	G	U
MOUSE μ	U	-	↓	-	-	-	-	A	C
HUMAN μ	C	-	↓	-	-	-	-	A	C
HAMSTER μ	C	-	↓	-	-	-	-	A	C
CHICKEN μ	G	-	↓	-	-	-	-	A	G
TOAD μ	U	-	↓	-	-	-	-	A	C
SHARK μ	C	-	↓	-	-	-	-	A	C
MOUSE α	G	-	↓	-	-	-	-	A	C
MOUSE γ_1	U	-	↓	-	-	-	-	A	-
MOUSE γ_{2a}	G	-	↓	-	-	-	-	A	-
MOUSE γ_{2b}	G	-	↓	-	-	-	-	A	-
MOUSE γ_3	U	-	↓	-	-	-	-	A	-
MOUSE ε	U	-	↓	-	-	-	-	C	A
MOUSE JH1	-	-	↓	-	-	-	-	-	C
JH2	-	-	↓	-	-	G	-	-	-
JH3	-	-	↓	-	-	G	-	-	-
JH4	-	-	↓	-	-	-	-	-	A
Cμ1	-	-	↓	-	-	-	-	-	A
Cμ2	C	-	↓	-	-	G	-	-	-
Cμ3	U	-	↓	-	-	-	G	-	-
μM1	-	-	↓	-	-	-	G	U	A

C

MOUSE μ	AGG	ACC	GUG	GAC	AAG	UCC	ACU	G↓GU	AAA	CCC	ACA	CUG	UAC	AAU	GUC
HUMAN μ	---	---	---	---	---	---	--C	-↓--	---	---	--C	---	---	--C	--G
HAMSTER μ	---	---	---	---	-G-	---	--C	-↓--	---	---	---	---	---	---	--A
CHICKEN μ	-A-	U-G	---	--U	-G-	G-U	U-G	-↓--	---	G-A	-GU	GCU	GU-	---	---
TOAD μ	---	-G-	A-U	---	---	--U	U--	-↓--	---	--U	--U	AAC	GUG	---	--G
SHARK μ	--A	--A	--U	A-U	--A	--G	-GC	-↓--	---	---	-GU	U-U	GUG	--C	A-U
MOUSE α	-A-	---	A-C	---	CGU	CUG	U-G	-↓--	---	---	--C	AAU	GU-	-GC	--G
MOUSE γ_1	-A-	-G-	C-C	UC-	C-C	--C	U--	-↓--	---	UGA	U-C	-A-	-GU	CC-	UGG
MOUSE γ_{2a}	-A-	-G-	U-C	UC-	CG-	A-U	C-G	-↓--	---	UGA	G-U	-A-	C--	CCA	CAA
MOUSE γ_{2b}	-A-	---	A-C	UC-	CG-	--U	C-G	-↓--	---	UGA	G-U	-A-	C--	CCA	CAA
MOUSE γ_3	-A-	-A-	C--	UCU	CGC	---	C--	-↓--	---	UGA	GA-	-A-	C--	CUA	-C-
MOUSE ε	-AA	--A	A-A	UC-	-CA	AG-	CU-	-↓--	--C	A--	U-C	--C	CGU	CCC	UC-

FIG. 5. Sequence comparison of immunoglobulin 5′ splice junctions. (A) The consensus 5′ splice junction sequence compared with the 5′ splice junction of the mouse Cμ4-to-M1 intron. Arrow designates the exon/intron boundary. The numbers give the frequency, in percent, with which a nucleotide is found at each position, based on an analysis of 1,446 splice junction sequences (46). (B) At the top, the consensus 5′ splice junction is shown base paired with U1 small nuclear RNA (59). In the middle, the 5′ regulatory splice junctions from phylogenetically conserved μ genes and other mouse immunoglobulin isotypes are shown. At the bottom, 5′ splice junctions of other introns within the mouse μ gene are shown. A dash signifys identity with the consensus nucleotide. (C) The sequence surrounding the 5′ regulatory splice junctions shown in panel B, spaced according to the translational reading frame. A dash signifys identity with the mouse μ sequence. Sources of the sequences are as follows: consensus (46), all mouse sequences (from GENBANK), human (32), hamster (31), chicken (12), toad (45), and shark (26).

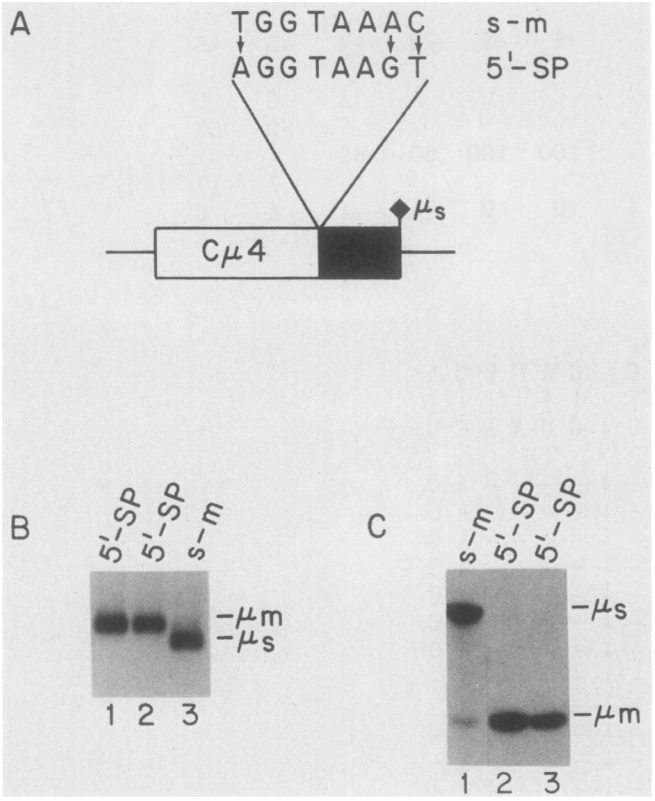

FIG. 6. Structure and expression of the 5'-SP mutation. (A) The sequence of the 5' splice junction of the mouse Cμ4-to-M1 intron (s-m) is shown above the sequence of the 5'-SP mutation. The nucleotide changes are identified with arrows. Symbols are as in Fig. 1B. (B) Northern blot analysis of poly(A)$^+$ RNA from S194 cells transfected with the plasmids shown above each lane; the transcripts are labeled. The blot was analyzed with a probe specific for SV40-*neo* sequences. Equal amounts of RNA were loaded in each lane, as was confirmed by a reprobe of this blot for polyomavirus expression (data not shown). (C) S1 nuclease analysis of RNA from S194 cells transfected with the plasmids shown above each lane. The S1 probe is diagrammed in Fig. 1D; the protected fragments are labeled. The RNAs in panel B, lanes 1 and 2, and panel C, lanes 2 and 3, are from two independent transfections.

general processing factors, is important in determining the in vivo μ_s/μ_m expression ratio. The poly(A) sites used here varied in strength: SVL and μ_m were the strongest, μ_s was intermediate, and α_s was the weakest. Replacement of the μ_m poly(A) site with this same set of poly(A) sites had no effect on μ_s expression, indicating that the μ_m site is not involved in a regulatory competition with the μ_s site in either early- or late-stage B cells. When the 5' splice junction of the Cμ4-to-M1 intron was mutated to match the consensus splice junction sequence, the splice reaction dominated over cleavage-polyadenylation at μ_s. Therefore, the reaction in competition with μ_s cleavage-polyadenylation must be splicing of Cμ4 to M1.

The analysis of a 5' splice junction point mutation that abolishes splicing of the Cμ4-to-M1 intron has been reported previously (50). Polyadenylation at μ_s was efficient with this mutant, and no polyadenylation at μ_m was detected. This result was interpreted to favor the μ_s site-splice model over the poly(A) site model. However, this interpretation is subject to the caveat that an RNA polyadenylated at μ_m but retaining the Cμ4-to-M1 intron might not be stable. Our protocol, in which the efficiency of the splicing reaction was increased rather than decreased, is not subject to such a caveat.

The effect of the 5'-SP mutation also demonstrated that the normal 5' splice junction is suboptimal with respect to splicing efficiency. This suboptimal sequence seems to be required to establish the proper regulatory balance between the splice and the competing (suboptimal) μ_s polyadenylation reaction. The evolutionary conservation of the suboptimal splice sequence is quite striking and strongly supports the idea that balanced processing reactions are critical to the regulatory mechanism.

In the context of the μ_s site-splice model, we suppose that the critical effect of decreasing the length of the Cμ4-to-M1 intron is to hasten the formation of the 3' splice junction and the commitment to splicing, thereby reducing the time available for effective cleavage-polyadenylation at the μ_s site. This idea was recently challenged by Galli et al. (19), who failed to observe an enhancement of μ_m mRNA production with constructs in which the Cμ4-to-M1 intron was shortened without appreciably altering the distance between the μ_s and μ_m poly(A) sites. However, the interpretation of these negative results is equivocal because there were no controls to demonstrate that the particular deletions and insertion used in these constructs did not diminish the splicing efficiency. These investigators also did not observe an increase in μ_s mRNA when they deleted the 3' splice junction of the Cμ4-to-M1 intron or the entire M1 exon. However, the interpretation of this result is complicated because Cμ4-to-M2 splicing occurs under these circumstances and could presumably compete effectively with the μ_s cleavage-polyadenylation reaction. In fact, when splicing was totally abolished by deletion of the 5' splice junction, a severalfold increase in μ_s mRNA was actually observed. Because of these ambiguities, we do not regard this evidence as being sufficiently compelling to reject the μ_s site-splice model.

Although some transcriptional termination between the μ_s and μ_m poly(A) sites occurs in plasmacytoma cells, several lines of evidence suggest that it did not contribute significantly to the results of our transfection experiments. In contrast to the experiments of Galli et al. (18), in which intron deletions resulted in a net gain of μ transcripts in a plasmacytoma cell, the effect we observed with intron deletion constructs was a decrease in μ_s-terminated RNA, which balanced the increase in μ_m expression. This effect was clearly observed with both the μ_s and the α_s poly(A) sites (Fig. 1 and 3), indicating that the deletion caused little or no change in the extent of transcription through this locus. Furthermore, if transcriptional termination prior to the μ_m poly(A) site were primarily responsible for the $\mu_s \gg \mu_m$ phenotype in plasmacytoma cells, then when the μ_s poly(A) site was replaced with the weaker α_s site, no change in μ_m expression would be expected. However, we observed a substantial increase in μ_m expression at the expense of μ_s* transcripts (Fig. 3A and B). This result could be explained in terms of transcriptional termination only if the extent of transcription were dependent on the frequency of processing at the μ_s poly(A) site. Indeed, processing at poly(A) sites has been shown to be required for transcriptional termination in some cases (11, 29, 56), and conceivably the location of the termination region could be coupled to the frequency of cleavage-polyadenylation. If this were the case, then the change in cleavage-polyadenylation frequency would be the primary level of control and transcriptional termination would be a secondary response. Clearly, transcription did

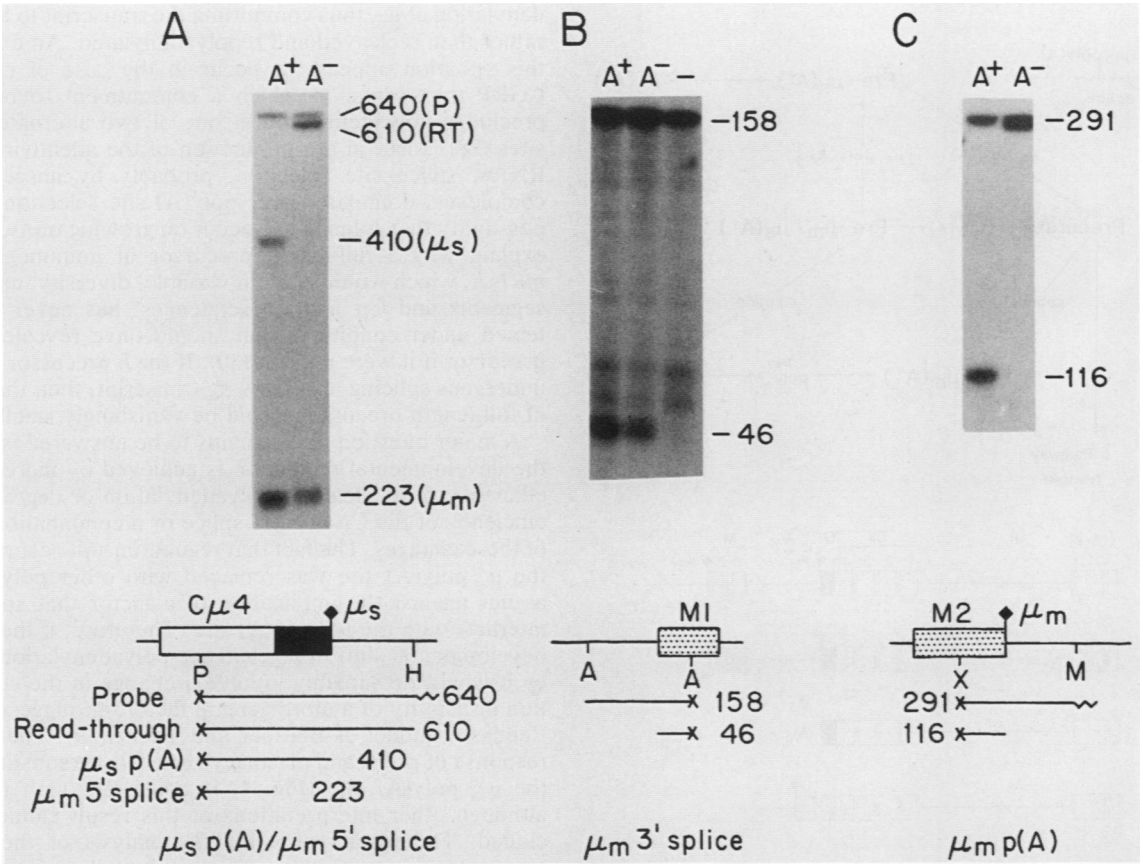

FIG. 7. S1 nuclease analysis of poly(A)$^+$ and poly(A)$^-$ nuclear RNA from the B-cell line 38C-13. For each panel, the RNA fraction analyzed [1 μg of poly(A)$^+$ and 100 μg of poly(A)$^-$] is shown above the lane; the S1 probes used and the resulting protected fragments are diagrammed below; the symbols used are the same as in Fig. 1, with the addition of restriction sites (H, *Hin*dIII; X, *Xba*I; A, *Ava*II; M, *Mbo*II). The lengths (in nucleotides) of the probes and protected fragments are indicated in the diagram and beside the corresponding gel bands. (A) S1 analysis with the μ_s p(A) site/μ_m 5′ splice junction probe. P, Probe; RT, read-through transcript. ∿, Vector sequences not homologous to intron sequences. (B) S1 analysis with the μ_m 3′ splice junction probe. A lane of carrier RNA only (−) is included. (C) S1 analysis with the μ_m poly(A) site probe.

not terminate prior to μ_m when the 5′-SP construct was expressed in the plasmacytoma cell, even though the μ_s poly(A) site and all downstream sequences remained intact.

On the basis of the idea that cleavage-polyadenylation at μ_s competes with splicing of the Cμ4-to-M1 exons, we suggest the processing scheme for μ mRNA shown in Fig. 8. We postulate that an unprocessed precursor, probably a nascent transcript, can undergo any of three processing events, and that the frequency with which each pathway is used determines the final μ_s/μ_m mRNA ratio. The existence of Pre-μ_s (A$^+$) and Pre-μ_m/μ_s(A$^+$), which are full-length precursors cleaved and polyadenylated at the μ_s and μ_m poly(A) sites, respectively (Fig. 8B), has been demonstrated previously by Northern blot analysis of nuclear poly(A)$^+$ mRNA (33). If the Pre-μ_m/μ_s(A$^+$) transcript undergoes the Cμ4-to-M1 splice, it is committed to producing mature μ_m mRNA. However, Pre-μ_m/μ_s(A$^+$) also retains the μ_s poly(A) site, and if it were recleaved and repolyadenylated at this site, it would then produce μ_s mRNA. The predicted product of such a processing reaction, an amputated transcript which extends from the μ_s cleavage site to the μ_m poly(A) site, has been detected in some cell lines (25, 33, 39). Since splicing of the exon containing the variable, diversity, and joining segments to the Cμ1 exon may frequently precede splicing of the Cμ4 and M1 exons (33), it has not been possible to detect Pre-μ_m(A$^+$) transcripts that have undergone splicing only of the Cμ4-to-M1 intron. The transcript Pre-μ_m(A$^-$), which has undergone the Cμ4-to-M1 splice prior to any cleavage-polyadenylation event and is thereby committed to producing μ_m mRNA (Fig. 8B), cannot be detected as a discrete component by Northern blot analysis because it has a heterogeneous 3′ end. However, a poly(A)$^-$ precursor transcript which has undergone the Cμ4-to-M1 splice was clearly detected by S1 nuclease protection analysis (Fig. 7). This component constituted a major fraction of the total μ_m mRNA precursor.

Although splicing reactions can occur independent of polyadenylation (20, 58), it has been assumed that polyadenylation generally precedes splicing. Nevins and Darnell (34) showed that in adenovirus mRNA, polyadenylation is an early processing event which normally precedes splicing. Furthermore, for many other genes, including the immunoglobulin genes, full-length precursor RNAs which have been polyadenylated but not yet spliced are detected. However, electron microscopic visualization of transcriptionally active chromatin has revealed that heterogeneous nuclear ribonucleoprotein particles occur at splice junction sequences and that they occasionally are seen to coalesce, forming an RNA loop. On more mature transcripts, these coalesced particles lose the intervening RNA loop in a process with properties

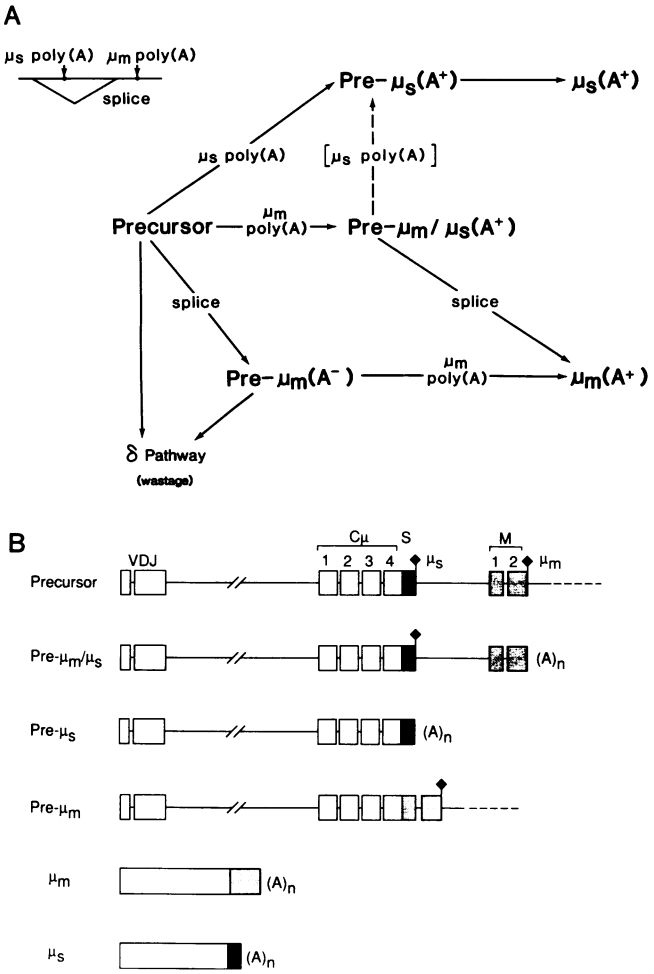

FIG. 8. Proposed processing scheme for heavy-chain immunoglobulin μ RNA and diagram of μ RNA precursor and product structures. (A) The diagram in the upper left illustrates the three processing options to which a μ precursor RNA can be subjected. The arrows in the processing scheme represent the processing events as labeled; the arrow with no label denotes splicing of nonregulatory introns. Although the pathway indicated by the dashed arrow and labeled [μ_s poly(A)] is known to exist (9, 12, 17), it is not clear to what extent it is used. The poly(A) symbols A^+ and A^- emphasize the 3′ end structures of the individual RNA species. (B) The structures of μ mRNA precursors and products. ▭, Exons common to both μ_m and μ_s mRNA; ▩, exons specific to μ_m mRNA; ▬, exons specific to μ_s mRNA; —, introns; ----, heterogeneous 3′ termini; ◆, poly(A) sites; $(A)_n$ represents cleaved and polyadenylated 3′ ends; VDJ refers to productively rearranged immunoglobulin variable, diversity, and joining segments; Cμ1-4 refers to the μ constant region exons; S and M refer to the secreted segment and membrane exons, respectively; and μ_s and μ_m refer to the secreted and membrane poly(A) sites, respectively.

similar to RNA splicing (6, 7, 36). Some of these heterogeneous nuclear ribonucleoprotein particles are bound by anti-small nuclear ribonucleoprotein antibodies (17), suggesting that they are splicing complexes analogous to the spliceosome complex (10). Although primary transcripts polyadenylated at the μ_m poly(A) site are present in pre-B and B cells, these transcripts may already contain a committed splice complex at the Cμ4 and M1 splice junctions. If this were the case, then the presence of the committed splice complex itself might be enough to preclude cleavage-polyadenylation at μ_s, thus committing the transcript to be spliced rather than recleaved and repolyadenylated. An example of this situation appears to occur in the case of calcitonin/CGRP transcripts, in which a commitment to be spliced precludes polyadenylation at one of two alternate poly(A) sites (28). Also, in the production of the adenovirus E3/L4 RNAs, splice site selection, probably by nascent splice complexes, dominates over poly(A) site selection (1). The possibility that splicing can occur on growing transcripts can explain why a full-length precursor of immunoglobulin δ mRNA, which would contain variable, diversity, and joining segments and Cμ and Cδ sequences, has never been detected under conditions that should have revealed such a precursor if it were present (30). If the δ precursor normally undergoes splicing as a growing transcript, then the amount of full-length precursor would be vanishingly small.

A major question that remains to be answered is whether the developmental regulation is achieved by increasing the efficiency of μ_s cleavage-polyadenylation or decreasing the efficiency of the Cμ4-to-M1 splice or a combination of both of these changes. The fact that regulation still occurred when the μ_s poly(A) site was replaced with other poly(A) sites argues against the implication of a factor that specifically interacts with the μ_s poly(A) site. Therefore, if there is any developmental shift in μ_s cleavage-polyadenylation efficiency,it would presumably involve a change in the concentration or activity of a more general factor, as suggested in the "endase" model of Blattner and Tucker (9). The different response of pre-B and plasmacytoma cells to substitutions at the μ_m poly(A) site (Fig. 4) is consistent with this idea, although other interpretations of this result cannot be excluded. The results of a kinetic analysis of the relative cleavage-polyadenylation efficiency in cell extracts from B cells and plasmacytomas were not supportive of this idea; the efficiency of μ_s and μ_m cleavage-polyadenylation in plasmacytomas appeared to be lower, rather than greater, than that in the B cells (55). However, the relevance of these in vitro data to the in vivo situation is unclear because this in vitro analysis was also unable to detect any difference in strength or affinity of the μ_s and μ_m poly(A) sites, which is contrary to our in vivo finding when the μ_s site was replaced by the μ_m site (Fig. 3).

Tsurushita and Korn (50, 51) have presented data which they interpret to indicate that splicing of Cμ4 to M1 is positively regulated in pre-B cells and inefficient in plasmacytoma cells. Our results do not conflict with this interpretation. However, splicing capacity cannot be completely limiting in plasmacytoma cells, since an increase in the spliced μ_m transcript was observed when the weak α_s poly(A) site was substituted for the μ_s poly(A) site in these cells. In addition, a μ_m message is efficiently processed in plasmacytoma cells when the μ_s poly(A) site is deleted from the primary transcript (13, 18, 37, 50). Therefore, if a positive-acting splice factor is present in B cells, it may act to stimulate splicing severalfold, but it cannot be absolutely required for splicing.

The type of regulatory model proposed here does not require a large change in the overall efficiency of either of the competing processing reactions as long as the affinities of the processed sites are appropriately tuned. Indeed, regulation typical of the wild-type μ gene was observed for the α_s-m and the m-m(Δ) constructs but was reduced in the other constructs. Moreover, all competitions between splice reactions and cleavage-polyadenylation reactions are not regulated in this way in lymphocytes. The human 2′-5′-oligoadenylate synthetase gene contains 3′-end-processing options

identical to those of the μ gene (5, 41). Yet when we compared the expression of this gene in human B and plasmacytoid cell lines, no difference was observed (unpublished results). The calcitonin/CGRP gene, although not identical in processing options to the μ gene, does contain a poly(A) site within an intron. When this gene was expressed in B cells, in contrast to μ gene expression, poly(A) site usage was completely dominant over the splicing reaction (28). Therefore, the affinity of the Cμ4 and M1 splice junctions for available splicing machinery, the affinity of the μ_s poly(A) site for available cleavage-polyadenylation machinery, and the spatial relationships between these sites must be delicately balanced to enable this gene to respond to changes which occur during B-cell maturation.

ACKNOWLEDGMENTS

This research was supported by Public Health Service grants from the National Institutes of Health (AI-17330, CA-06927) and by an appropriation from the Commonwealth of Pennsylvania. M.L.P. acknowledges a fellowship from the American Cancer Society.

LITERATURE CITED

1. **Adami, G., and J. R. Nevins.** 1988. Splice site selection dominates over poly(A) site choice in RNA production from complex adenovirus transcription units. EMBO J. **7**:2107–2116.
2. **Alt, F. W., A. L. M. Bothwell, M. Knapp, E. Siden, E. Mather, M. Koshland, and D. Baltimore.** 1980. Synthesis of secreted and membrane-bound immunoglobulin μ heavy chains is directed by mRNAs that differ at their 3′ ends. Cell **20**:293–301.
3. **Alt, F. W., N. Rosenberg, S. Lewis, E. Thomas, and D. Baltimore.** 1981. Organization and reorganization of immunoglobulin genes in A-MuLV transformed cells—rearrangement of heavy but not light chain genes. Cell **27**:381–390.
4. **Atchison, M. L., and R. P. Perry.** 1986. Tandem kappa immunoglobulin promoters are equally active in the presence of the kappa enhancer: implications for models of enhancer function. Cell **46**:253–262.
5. **Benech, P., G. Merlin, M. Revel, and J. Chebath.** 1985. 3′ end structure of the human (2′-5′) oligo A synthetase gene: prediction of two distinct proteins with cell type-specific expression. Nucleic Acids Res. **13**:1267–1281.
6. **Beyer, A. L., A. H. Bouton, and O. L. Miller, Jr.** 1981. Correlation of hnRNP structure and nascent transcript cleavage. Cell **26**:155–165.
7. **Beyer, A. L., and Y. N. Osheim.** 1988. Splice site selection, rate of splicing, and alternative splicing on nascent transcripts. Genes Dev. **2**:754–765.
8. **Birnstiel, M. L., M. Busslinger, and K. Strub.** 1985. Transcription termination and 3′ processing: the end is in site! Cell **41**:349–359.
9. **Blattner, F. R., and P. W. Tucker.** 1984. The molecular biology of immunoglobulin D. Nature (London) **307**:417–422.
10. **Brody, E., and J. Abelson.** 1985. The "spliceosome": yeast premessenger RNA associates with a 40S complex in a splicing-dependent reaction. Science **228**:963–967.
11. **Connelly, S., and J. L. Manley.** 1988. A functional mRNA polyadenylation signal is required for transcription termination by RNA polymerase II. Genes Dev. **2**:440–452.
12. **Dahan, A., C.-A. Reynaud, and J.-C. Weill.** 1983. Nucleotide sequence of the constant region of a chicken μ heavy chain immunoglobulin mRNA. Nucleic Acids Res. **11**:5381–5389.
13. **Danner, D., and P. Leder.** 1985. Role of an RNA cleavage/poly(A) addition site in the production of membrane-bound and secreted IgM mRNA. Proc. Natl. Acad. Sci. USA **82**:8658–8662.
14. **DeChiara, T. M., F. Erlitz, and S. J. Tarnowski.** 1986. Procedures for *in vitro* DNA mutagenesis of human leukocyte interferon sequences. Methods Enzymol. **119**:403–415.
15. **Early, P., J. Rogers, M. Davis, K. Calame, M. Bond, R. Wall, and L. Hood.** 1980. Two mRNAs can be produced from a single immunoglobulin μ gene by alternative RNA processing pathways. Cell **20**:313–319.
16. **Eperon, L. P., J. P. Estibeiro, and I. C. Eperon.** 1986. The role of nucleotide sequences in splice site selection in eukaryotic pre-messenger RNA. Nature (London) **324**:280–283.
17. **Fakan, S., G. Leser, and T. E. Martin.** 1986. Immunoelectron microscope visualization of nuclear ribonucleoprotein antigens within spread transcription complexes. J. Cell. Biol. **103**:1153–1157.
18. **Galli, G., J. W. Guise, M. A. McDevitt, P. W. Tucker, and J. R. Nevins.** 1987. Relative position and strengths of poly(A) sites as well as transcription termination are critical to membrane versus secreted μ-chain expression during B-cell development. Genes Dev. **1**:471–481.
19. **Galli, G., J. Guise, P. W. Tucker, and J. R. Nevins.** 1988. Poly(A) site choice rather than splice site choice governs the regulated production of IgM heavy-chain RNAs. Proc. Natl. Acad. Sci. USA **85**:2439–2443.
20. **Green, M. R., T. Maniatis, and D. A. Melton.** 1983. Human β-globin pre-mRNA synthesized *in vitro* is accurately spliced in Xenopus oocyte nuclei. Cell **32**:681–694.
21. **Grosschedl, R., and D. Baltimore.** 1985. Cell-type specificity of immunoglobulin gene expression is regulated by at least three DNA sequence elements. Cell **41**:885–897.
22. **Guise, J. W., P. L. Lim, D. Yuan, and P. W. Tucker.** 1988. Alternative expression of secreted and membrane forms of immunoglobulin μ-chain is regulated by transcriptional termination in stable plasmacytoma transfectants. J. Immunol. **140**:3988–3994.
23. **Kelley, D. E., and R. P. Perry.** 1986. Transcriptional and post-transcriptional control of immunoglobulin mRNA production during B lymphocyte development. Nucleic Acids Res. **14**:5431–5447.
24. **Kelley, D. E., B. A. Pollok, M. L. Atchison, and R. P. Perry.** 1988. The coupling between enhancer activity and hypomethylation of κ immunoglobulin genes is developmentally regulated. Mol. Cell. Biol. **8**:930–937.
25. **Kemp, D., G. Morahan, A. F. Cowman, and A. W. Harris.** 1983. Production of RNA for secreted immunoglobulin μ chains does not require transcriptional termination 5′ to the μ_m exons. Nature (London) **301**:84–86.
26. **Kokubu, F., K. Hinds, R. Litman, M. J. Shamblott, and G. W. Litman.** 1988. Complete structure and organization of immunoglobulin heavy chain constant region genes in a phylogenetically primitive vertebrate. EMBO J. **7**:1979–1988.
27. **Law, R., M. D. Kuwabara, M. Briskin, N. Fasel, G. Hermanson, D. S. Sigman, and R. Wall.** 1987. Protein-binding site at the immunoglobulin $\mu_{membrane}$ polyadenylation signal: possible role in transcription termination. Proc. Natl. Acad. Sci. USA **84**:9160–9164.
28. **Leff, S. E., R. M. Evans, and M. G. Rosenfeld.** 1987. Splice commitment dictates neuron-specific alternative RNA processing in calcitonin/CGRP gene expression. Cell **48**:517–524.
29. **Logan, J., E. Falck-Pedersen, J. E. Darnell, Jr., and T. Shenk.** 1987. A poly(A) addition site and a downstream termination region are required for efficient cessation of transcription by RNA polymerase II in the mouse β^{maj}-globin gene. Proc. Natl. Acad. Sci. USA **84**:8306–8310.
30. **Mather, E. L., K. J. Nelson, J. Haimovich, and R. P. Perry.** 1984. Mode of regulation of immunoglobulin μ- and δ-chain expression varies during B-lymphocyte maturation. Cell **36**:329–338.
31. **McGuire, K. L., W. R. Duncan, and P. W. Tucker.** 1985. Phylogenetic conservation of immunoglobulin heavy chains: direct comparison of hamster and mouse Cμ genes. Nucleic Acids Res. **13**:5611–5628.
32. **Milstein, C. P., E. V. Deverson, and T. H. Rabbitts.** 1984. The sequence of the human immunoglobulin μ-δ intron reveals possible vestigial switch segments. Nucleic Acids Res. **12**:6523–6535.
33. **Nelson, K. J., J. Haimovich, and R. P. Perry.** 1983. Characterization of productive and sterile transcripts from the immunoglobulin heavy-chain locus: processing of μ_m and μ_s mRNA. Mol. Cell. Biol. **3**:1317–1332.

34. **Nevins, J. R., and J. E. Darnell, Jr.** 1978. Steps in the processing of Ad2 mRNA: poly(A)$^+$ nuclear sequences are conserved and poly(A) addition precedes splicing. Cell **15**:1477–1493.
35. **Ochi, A., R. G. Hawley, T. Hawley, M. J. Shulman, A. Traunecker, G. Köhler, and N. Hozumi.** 1983. Functional immunoglobulin M production after transfection of cloned immunoglobulin heavy and light chain genes into lymphoid cells. Proc. Natl. Acad. Sci. USA **80**:6351–6355.
36. **Osheim, Y. N., O. L. Miller, Jr., and A. L. Beyer.** 1985. RNP particles at splice junction sequences on Drosophila chorion transcripts. Cell **43**:143–151.
37. **Peterson, M. L., and R. P. Perry.** 1986. Regulated production of μ_m and μ_s mRNA requires linkage of the poly(A) addition sites and is dependent on the length of the μ_s-μ_m intron. Proc. Natl. Acad. Sci. USA **83**:8883–8887.
38. **Reddy, V. B., B. Thimmappaya, R. Dhar, K. N. Subramanian, S. Zain, J. Pan, P. K. Ghosh, M. L. Celma, and S. M. Weissman.** 1978. The genome of simian virus 40. Science **200**:494–502.
39. **Rogers, J., N. Fasel, and R. Wall.** 1986. A novel RNA in which the 5′ end is generated by cleavage at the poly(A) site of immunoglobulin heavy-chain secreted mRNA. Mol. Cell. Biol. **6**:4749–4752.
40. **Ruether, J. E., A. Maderious, D. Lavery, J. Logan, S. Man Fu, and S. Chen-Kiang.** 1986. Cell-type-specific synthesis of murine immunoglobulin μ RNA from an adenovirus vector. Mol. Cell. Biol. **6**:123–133.
41. **Saunders, M. E., D. R. Gewert, M. E. Tugwell, M. McMahon, and B. R. G. Williams.** 1985. Human 2-5A synthetase: characterization of a novel cDNA and corresponding gene structure. EMBO J. **4**:1761–1768.
42. **Scherrer, K.** 1969. Isolation and sucrose gradient analysis of RNA, p. 413–432. *In* K. Habel and N. Salzman (ed.), Fundamental techniques in virology. Academic Press, Inc., New York.
43. **Schibler, U., K. B. Marcu, and R. P. Perry.** 1978. The synthesis and processing of the messenger RNAs specifying heavy and light chain immunoglobulins in MPC-11 cells. Cell **15**:1495–1509.
44. **Schibler, U., T. Wyler, and O. Hagenbuchle.** 1975. Changes in size and secondary structure of the ribosomal transcription unit during vertebrate evolution. J. Mol. Biol. **94**:503–517.
45. **Schwager, J., C. A. Mikoryak, and L. A. Steiner.** 1988. Amino acid sequence of heavy chain from *Xenopus laevis* IgM deduced from cDNA sequence: implications for evolution of immunoglobulin domains. Proc. Natl. Acad. Sci. USA **85**:2245–2249.
46. **Shapiro, M. B., and P. Senapathy.** 1987. RNA splice junctions of different classes of eukaryotes: sequence statistics and functional implications in gene expression. Nucleic Acids Res. **15**:7155–7174.
47. **Sharp, P. A.** 1987. Splicing of messenger RNA precursors. Science **235**:766–771.
48. **Solnick, D.** 1981. An adenovirus mutant defective in splicing RNA from early region 1A. Nature (London) **291**:508–511.
49. **Treisman, R., S. H. Orkin, and T. Maniatis.** 1983. Specific transcription and RNA splicing defects in five cloned β-thalassaemia genes. Nature (London) **302**:591–596.
50. **Tsurushita, N., N. M. Avdalovic, and L. J. Korn.** 1987. Regulation of differential processing of mouse immunoglobulin μ heavy-chain mRNA. Nucleic Acids Res. **15**:4603–4615.
51. **Tsurushita, N., L. Ho, and L. J. Korn.** 1988. Nuclear factors in B lymphoma enhance splicing of mouse membrane-bound μ mRNA in *Xenopus* oocytes. Science **239**:494–497.
52. **Tsurushita, N., and L. J. Korn.** 1987. Effects of intron length on differential processing of mouse μ heavy-chain mRNA. Mol. Cell. Biol. **7**:2602–2605.
53. **Tucker, P. W., J. L. Slightom, and F. R. Blattner.** 1981. Mouse IgA heavy chain gene sequence: implications for evolution of immunoglobulin hinge exons. Proc. Natl. Acad. Sci. USA **78**:7684–7688.
54. **Van Ness, B. G., M. Weigert, C. Coleclough, E. L. Mather, D. E. Kelley, and R. P. Perry.** 1981. Transcription of the unrearranged mouse C_κ locus: sequence of the initiation region and comparison of activity with a rearranged V_κ-C_κ gene. Cell **27**:593–602.
55. **Virtanen, A., and P. A. Sharp.** 1988. Processing at immunoglobulin polyadenylation sites in lymphoid cell extracts. EMBO J. **7**:1421–1429.
56. **Whitelaw, E., and N. Proudfoot.** 1986. α-Thalassaemia caused by a poly(A) site mutation reveals that transcriptional termination is linked to 3′ end processing in the human α2 globin gene. EMBO J. **5**:2915–2922.
57. **Yuan, D., and P. W. Tucker.** 1984. Transcriptional regulation of the μ-δ heavy chain locus in normal murine B lymphocytes. J. Exp. Med. **160**:564–583.
58. **Zeevi, M., J. R. Nevins, and J. E. Darnell.** 1981. Nuclear RNA is spliced in the absence of poly(A) addition. Cell **26**:39–46.
59. **Zhuang, Y., H. Leung, and A. M. Weiner.** 1987. The natural 5′ splice site of simian virus 40 large T antigen can be improved by increasing the base complementarity to U1 RNA. Mol. Cell. Biol. **7**:3018–3020.
60. **Zhuang, Y., and A. M. Weiner.** 1986. A compensatory base change in U1 snRNA suppresses a 5′ splice mutation. Cell **46**:827–835.